Beyond the Heisenberg Model: Anisotropic Exchange Interaction between a Cu-Tetraazaporphyrin Monolayer and $Fe_3O_4(100)$

J. Klanke,[1] E. Rentschler,[1] K. Medjanik,[2] D. Kutnyakhov,[2] G. Schönhense,[2] S. Krasnikov,[3] I. V. Shvets,[3] S. Schuppler,[4] P. Nagel,[4] M. Merz,[4] and H. J. Elmers[2,*]

[1]*Institut für Anorganische Chemie und Analytische Chemie, Johannes Gutenberg-Universität Mainz, D-55099 Mainz, Germany*
[2]*Institut für Physik, Johannes Gutenberg-Universität Mainz, D-55128 Mainz, Germany*
[3]*Centre for Research on Adaptive Nanostructures and Nanodevices (CRANN), School of Physics, Trinity College Dublin, Dublin 2, Republic of Ireland*
[4]*Karlsruhe Institute of Technology, Institut für Festkörperphysik (IFP), D-76021 Karlsruhe, Germany*

(Received 29 June 2012; published 25 March 2013)

The exchange coupling of a single spin localized at the central ion of Cu-tetraazaporphyrin on a magnetite(100) surface has been studied using x-ray magnetic circular dichroism (XMCD). Sum rule analysis of the XMCD spectra results in Cu spin and orbital magnetic moments as a function of the applied external field at low temperatures (20 K). The exchange coupling is positive for magnetization direction perpendicular to the surface (ferromagnetic) while it is negative for in-plane magnetization direction (antiferromagnetic). We attribute the anisotropy of the Heisenberg exchange coupling to an orbitally dependent exchange Hamiltonian.

DOI: 10.1103/PhysRevLett.110.137202 PACS numbers: 75.70.−i, 33.15.Kr, 75.30.Et, 78.70.Dm

The Heisenberg exchange coupling is one of the most popular models for the description of the magnetic coupling on a quantum-mechanical basis. It is particularly important for molecular magnets where Heisenberg coupling shows a fascinatingly rich behavior [1,2], with potential applications as memory storage on the molecular level [3], quantum calculators [4,5], and as building blocks of spintronic devices [6].

Usually the exchange coupling is described by a pure spin Hamiltonian with an isotropic exchange constant, depending on the distance of the coupled spins and on the contributing orbitals but not on the spin direction itself. Only very recently, a study of the exchange interaction in molecular magnets with unquenched orbital angular momenta describes the exchange interaction by an orbitally dependent exchange Hamiltonian, which is equivalent to an anisotropic Heisenberg exchange constant [1]. An anisotropic coupling of a single magnetic moment comprising a large orbital moment has been reported for Tb-phthalocyanine coupled to a ferromagnetic substrate [7]. Previous investigations of the exchange coupling between molecules and ferromagnetic surfaces [8–13] revealed a rather strong coupling aligning the molecular spin either parallel or antiparallel to the ferromagnetic surface. The dependence of the coupling on the magnetization direction was explicitly studied by Wende *et al.* [14] for Fe-porphyrin on Ni(100) with the result of an isotropic interaction.

In this Letter, we investigate the angular dependence of the exchange coupling for a single molecular spin of an unpaired Cu *d* electron in Cu-tetraazaporphyrin with 8 4-tert-butylphenyl substituents (Cu4Dinit) to a ferrimagnetic magnetite surface. Porphyrins are important stable building blocks of molecules used as well in organic electronics and in biology. We have chosen Cu as the central metal atom because the single unoccupied *d* state provides the simplest model system, while multiple unpaired spins will likely show anisotropic coupling, too. The relatively large tert-butylphenyl substituents inhibit an additional intermolecular magnetic interaction that is unwanted in our case. In addition, they support a flat orientation of the molecule with the Cu spin in close contact with the surface.

The heterogeneous coupling of a paramagnetic spin to a strong ferromagnet with a coupling strength of the same order as the external field is an important precondition for an unambiguous determination of the directional dependence of the exchange coupling. We manipulate the magnetization direction of the magnetite film by a sufficiently large external field in a well-defined direction. Then, the magnitude of the induced paramagnetic Cu moment, as determined by element-specific magnetometry, measures the coupling strength as an additive effective field. For the investigated system we find a ferromagnetic coupling for perpendicular magnetization while it is antiferromagnetic for in-plane magnetization (see Fig. 1).

The samples were prepared by molecular beam epitaxy of Cu4Dinit on $Fe_3O_4(100)/MgO(100)$ films in ultrahigh vacuum. The coverage was 0.5 ± 0.2 monolayer (ML). X-ray magnetic circular dichroism (XMCD) measurements were carried out at IFP's soft x-ray beam line WERA at the Karlsruhe synchrotron light source ANKA, using the XMCD setup of the Max Planck Institute for Intelligent Systems, Stuttgart. X-ray absorption spectra (XAS) were determined from the total electron yield as measured by the sample current at a constant temperature of 20 K. A magnetic field of up to 4.5 T was applied parallel to the incident

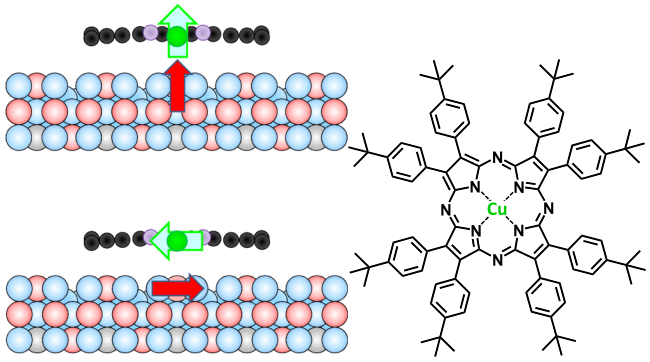

FIG. 1 (color online). Sketch of the anisotropic exchange coupling of the Cu spin in Cu4Dinit to the octahedral Fe spin in the $Fe_3O_4(100)$ surface. The $Fe_3O_4(100)$ surface structure is adapted from Ref. [28].

photon beam with the sample normal oriented either parallel to the magnetic field or at an angle of 55°. The energy resolution of the x-ray monochromator was adjusted to 0.4 eV. The polarization degree is $P = 0.87$ at the Cu L edge. Even after several days of absorption measurements we did not detect any changes of the spectra indicating that no radiation damage of the molecules occurred.

Figures 2 and 3 show XAS and XMCD spectra for the Cu4Dinit/Fe_3O_4 monolayer measured with the circularly polarized photon beam parallel to the surface normal and at an angle of incidence of 55°. Data measured for a powder sample are shown for comparison. The background signal comprising transitions into continuous states and absorption at lower energy absorption edges has been subtracted.

For the polycrystalline Cu4Dinit powder the relative alignment of the molecule's symmetry axis and the x-ray beam is random. [15] According to previous results [16–20] obtained for Cu-phthalocyanine (CuPc), the XAS spectrum comprises two main peaks at the L_3 and L_2 edge, respectively. The two main peaks indicate transitions from the spin-orbit split $2p$ states into the single $3d$ hole with mainly $d_{x^2-y^2}$ character. Two post-edge satellite peaks (labeled $A1$ and $A2$) show up at higher photon energies (3.5 and 7.3 eV above the main peaks).

The off-normal XAS data for the Cu4Dinit monolayer show similar features with slightly reduced satellite peaks. This is in contrast to a CuPc monolayer adsorbed on metallic Ag [21] where peaks $A1$ and $A2$ are completely quenched. With the radiation impinging at normal incidence, we observe considerably suppressed satellite peaks in comparison to the main line transition.

The origin of the satellite peaks has been assigned to transitions into $e_g(\pi^*)$ states with $d_{xz,yz}$ character ($A1$) and $a_{1g}(3d_{z^2-r^2})$ states ($A2$). [18] In Ref. [20], satellites $A1$, $A2$ and also a third satellite at 11 eV above the edge are attributed to a combination of Cu $3d$, $4s$ states and N $2p$ states. Charge transfer multiplet calculations [22] considering a weak charge transfer from the metal ion to the ligands also produce a satellite peak at 3.5 eV above the main line, indicating the contribution of many-particle final state effects. The main line transition into the $d_{x^2-y^2}$

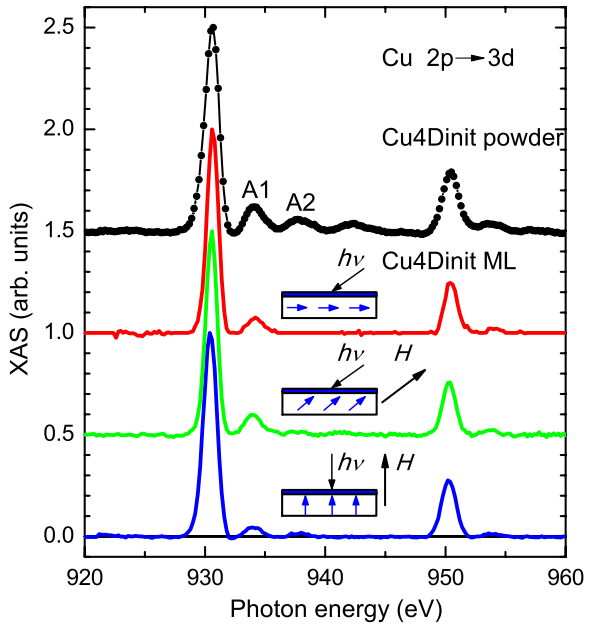

FIG. 2 (color online). XAS intensity at 20 K for circular polarization at the Cu $2p \rightarrow 3d$ transition normalized to the maximum. Insets indicate (from top to bottom) Cu4Dinit powder sample, Cu4Dinit ML measured for the remanent state of the magnetite film without applied field, Cu4Dinit ML measured with external field of 4.5 T applied at an angle of 55° with respect to the normal, and Cu4Dinit ML measured with external field of 1.2 T applied perpendicular to the surface.

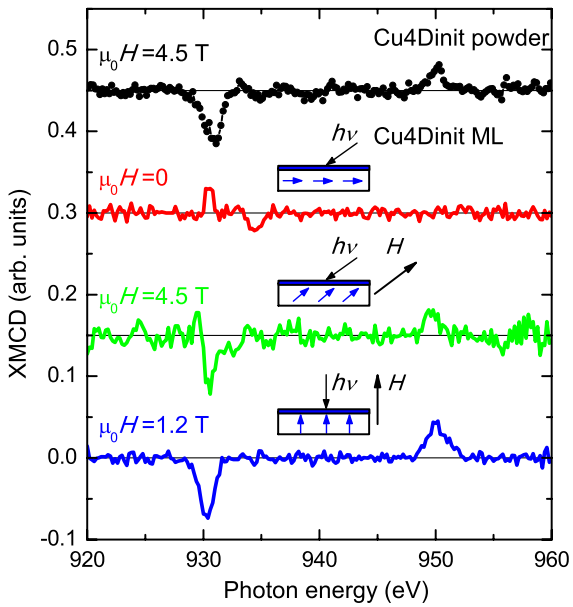

FIG. 3 (color online). XMCD calculated from the difference of XAS data measured with parallel and antiparallel orientation of magnetic field and photon spin. Same series of measurements as in Fig. 2.

state is expected to be large when the electric field vector lies in the plane of the molecule, and to be small for the perpendicular direction. The opposite behavior is expected for the $A1$ satellite. Thus, the angular dependence of the XAS spectra indicates that the Cu4Dinit molecules are not randomly oriented. The decrease of the relative intensity of the $A1$ satellite and the main L_3 peak for normal incidence is consistent with a flat orientation of the molecules in agreement with CuPc on metallic Ag [21] and on high quality oxidic surfaces like $TiO_2(110)$ [23].

Figure 4 visualizes the sum rule analysis that is applied to quantify the magnetic moment localized at the Cu ion. Figure 4(a) shows the $2p \rightarrow 3d$ XAS spectra I^+ and I^- for Cu in the Cu4Dinit monolayer as determined from data measured with the incident beam and external field direction oriented parallel to the film normal. Both spectra represent an average of a dozen spectra acquired with opposite magnetization and polarization directions. Figure 4(b) shows the corresponding XMCD spectrum $I^+ - I^-$ and the integrated XMCD spectrum. Peaks with opposite signs in the XMCD spectrum at the L_3 and L_2 edges indicate that the total magnetic moment is dominated by the spin contribution. The spin and orbital momentum, μ_{spin} and μ_{orb}, projected on to the incident x-ray beam is calculated by [24]

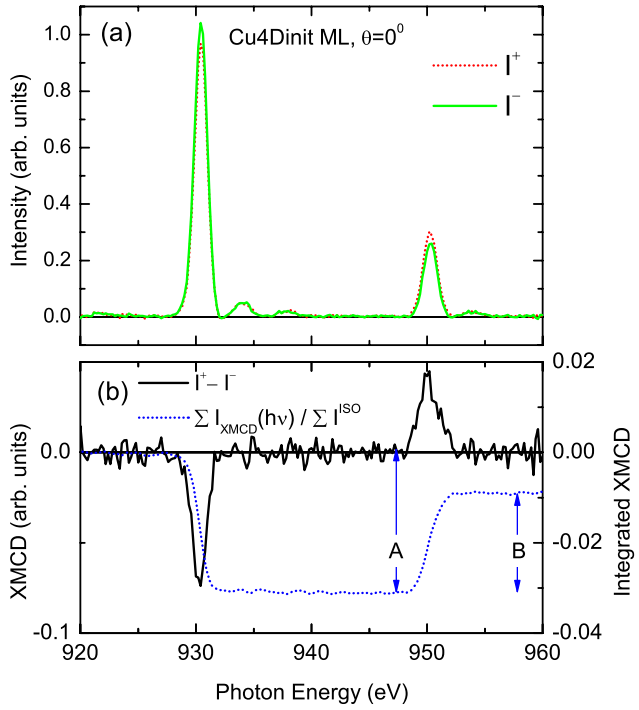

FIG. 4 (color online). Cu $2p \rightarrow 3d$ XAS and XMCD spectra measured for the Cu4Dinit ML on magnetite. (a) Solid (dashed) ($I^{+(-)}$) lines show the XAS spectra measured with external field 1.2 T applied parallel (antiparallel) to the surface normal and to the spin of the incident photon beam. (b) Full ($I^+ - I^-$) and dotted ($\sum I_{\text{XMCD}} / \sum I^{\text{ISO}}$) lines represent the XMCD and its integrated spectrum normalized to the isotropic energy-integrated x-ray absorption.

$$\mu_{\text{spin}}^{\text{eff}} = \mu_{\text{spin}} + 7\langle T\rangle\mu_B = -\frac{3A - 6B}{I^{\text{ISO}}}\frac{n_h\mu_B}{P}, \quad (1)$$

$$\mu_{\text{orb}} = -\frac{A + B}{I^{\text{ISO}}}\frac{2n_h\mu_B}{P}, \quad (2)$$

where A and B denote integrals of the XMCD spectrum at the L_3 and L_2 edges and I^{ISO} corresponds to the isotropic energy-integrated XAS intensity, $(I^+ + I^- + I^0)$, n_h represents the number of d holes which is assumed as $n_h = 1$ for the present case, neglecting small deviations due to charge transfer or hybridization, and P is the degree of circular polarization. $\langle T\rangle$ is the magnetic dipole operator that measures the quadrupole moment of the spin operator. For the powder sample and measurements with the angle of incidence set to the magic angle $\theta = 55°$, the absorption intensity for linear polarization parallel to the magnetization, I^0, is set to $(I^+ + I^-)/2$ and $\langle T\rangle$ is approximately zero even for the nonvanishing spin-orbit coupling for the magnetic field applied along 55°. In the case of normal incidence, I^0 vanishes for flatly adsorbed molecules. According to results for CuPc/Ag(100) [21] the dipole operator is $7\langle T\rangle\mu_B = 1.88\ \mu_{\text{spin}}$ and $7\langle T\rangle\mu_B = -0.95\ \mu_{\text{spin}}$ for magnetization pointing normal and parallel to the surface, respectively.

Results from the sum rule analysis are summarized in Table I. For the powder sample we assume that a coupling between the molecular moments can be neglected as confirmed by standard magnetometry. Then, the thermal average of a magnetic moment μ_T with total angular momentum $j = 1/2$ is calculated by $\mu_T/\mu_B = \tanh(\mu_B\mu_0 H/k_B T)$, neglecting spin-orbit coupling. Thus, at $T = 20$ K and external field $\mu_0 H = 4.5$ T we expect a value of $\mu_T = 0.15\ \mu_B$, in good agreement with the experimentally observed value.

For the experimental conditions of the XMCD experiment, the Brillouin function can be linearized, resulting in a magnetic susceptibility $\chi_T/\mu_0 = \mu_B^2/k_B T$. For the powder sample we find an experimental value $\chi_T/\mu_0 = 0.0334\ \mu_B \text{T}^{-1}$. For the Cu4Dinit monolayer and $\theta = 0°$, one therefore expects an induced moment of $\mu_{\text{sum}}(\theta, H) = \chi_T H = 0.040\ \mu_B$, which is considerably smaller than the observed value. We attribute the difference to an additional ferromagnetic coupling between the substrate magnetization and the molecular moment, which is described by an additive effective coupling field $H_{c,\perp}$: $\mu_{\text{sum}}(0, H) = \chi_T(H + H_{c,\perp})$, resulting in $\mu_0 H_{c,\perp} = (2.1 \pm 0.6)$ T.

The magnetite magnetization is aligned with the external field for fields exceeding its saturation magnetization of $J_s = 0.65$ T. Projecting the substrate magnetization and the corresponding coupling field onto a normal and an in-plane component, respectively, we obtain

$$\mu_{\text{sum}}(\theta, H) = \chi_T(H + H_{c,\perp}\cos^2\theta + H_{c,\parallel}\sin^2\theta), \quad (3)$$

for the case of a large field applied at an angle θ. For the remanent case the magnetite magnetization lies parallel to the surface in the direction defined by the previously

TABLE I. Sum rule results for $n_h = 1$. The spin moment is calculated by $\mu_{\text{spin}} = \mu_{\text{spin}}^{\text{eff}}/(1 + 7\langle T\rangle\mu_B/\mu_{\text{spin}})$. The statistical error is indicated in brackets.

Sample	θ	$\mu_0 H$ (T)	$\mu_{\text{spin}}^{\text{eff}}$ (μ_B)	μ_{spin} (μ_B)	μ_{orb} (μ_B)	μ_{sum} (μ_B)
Powder		4.5	0.14(1)	0.14(1)	0.01(1)	0.15(1)
Monolayer	55°	0.0	0.00(1)	0.0(1)	0.00(1)	0.0(1)
Monolayer	55°	4.5	0.12(1)	0.12(1)	0.01(1)	0.13(1)
Monolayer	0°	1.2	0.26(2)	0.09(1)	0.02(1)	0.11(1)

applied field as proven by XMCD at the Fe L edges (see the Supplemental Material [25]). Consequently, the induced Cu moment is given by

$$\mu_{\text{sum}}(\theta, 0) = \chi_T(H_{c,\parallel}\sin\theta). \quad (4)$$

For an isotropic exchange coupling, one expects $H_{c,\perp} = H_{c,\parallel}$ and Eq. (3) would result in $\mu_{\text{sum}} = 0.22\ \mu_B$. Instead, we observe a much smaller value ($0.13\ \mu_B$) for the magnetic field applied along 55°. This smaller value can only be explained by a negative (antiferromagnetic) coupling field for the in-plane component, corresponding to $\mu_0 H_{c,\parallel} = -(2 \pm 1)$ T, that partly compensates the positive (ferromagnetic) out-of-plane coupling field.

An alternative explanation for a negative coupling field could be a strong uniaxial magnetic anisotropy favoring the perpendicular magnetization direction. A perpendicular anisotropy is in accordance with the observed decrease of the orbital magnetic moment with increasing angle θ [26], although it would be too small to explain our results. The decrease of the orbital moment with increasing angle θ was also observed for the related molecule Cu-phthalocyanine on Cu [21], without a magnetic anisotropy. As pointed out in Ref. [21], no single-ion magnetic anisotropy should exist for a pure $S = 1/2$ system. Consequently, the orbital moment anisotropy was explained by a different admixture of excited states for in-plane and out-of-plane moments due to spin-orbit coupling instead of a magnetic anisotropy in the ground state. Therefore, we assume that the magnetic anisotropy can be neglected in our case.

In the remanent case the magnetic dipole operator is antiparallel to the spin moment and the effective spin moment is expected to be almost zero. This is confirmed by the sum rule analysis of the corresponding XMCD spectrum (see Fig. 5). The differential XMCD spectrum, however, does not vanish completely. The fact that the spectral features of the magnetic dipole term and of the spin moment may considerably differ and therefore do not cancel each other for in-plane magnetization was pointed out in Ref. [27]. We take the positive XMCD peak at the leading L_3 edge as a hint to an opposite direction of the Cu moment corresponding to an antiparallel coupling field in qualitative agreement with the previously determined negative value of the coupling field. The additional negative peak at the position of the A1 satellite might be attributed to a very strong hybridization of the Cu $3d_{xz,yz}$ states with the adjacent orbitals in the case of planar magnetization. The increased lifetime broadening quenches these features at the L_2 edge.

The Hamiltonian describing a coupling depending on the spin direction can be written as

$$H = -J_\perp \sum_{\langle i,j\rangle} S_{z,i}S_{z,j} - J_\parallel \sum_{\langle i,j\rangle} (S_{x,i}S_{x,j} + S_{y,i}S_{y,j}). \quad (5)$$

The spin of the Fe ion may be estimated as $S_j = 2$ and that of the Cu ion as $S_i = 1/2$. The corresponding coupling constants are $J_\perp = +(0.12 \pm 0.03)$ meV and $J_\parallel = -(0.11 \pm 0.05)$ meV. For $J_\perp = -2J_\parallel$, Eq. (5) is equivalent to dipolar coupling. However, absolute values of the dipolar coupling assuming a distance of 2 Å of two moments with 1 μ_B and 4 μ_B results in $J_\perp = 0.05$ meV

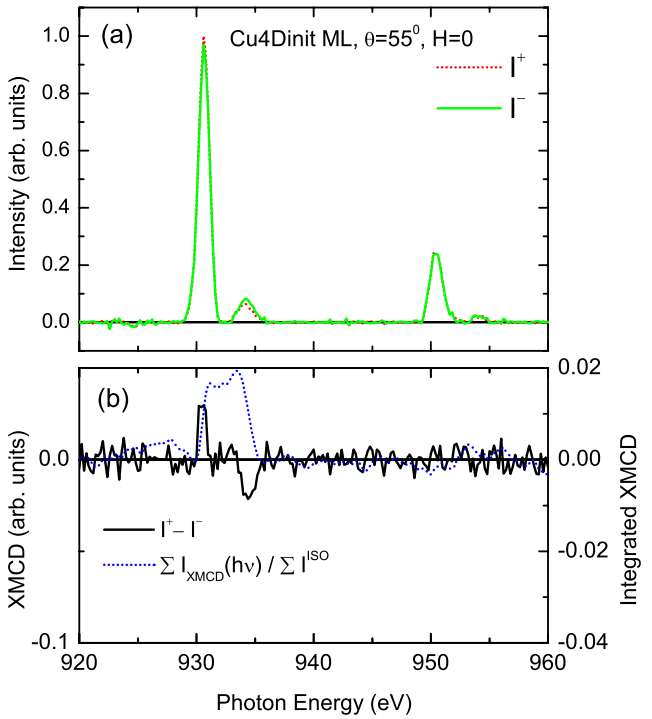

FIG. 5 (color online). Cu $2p \rightarrow 3d$ XAS and XMCD spectra measured for the Cu4Dinit ML on magnetite at 55° angle of incidence of the photon beam. (a) Solid (dashed) ($I^{+(-)}$) lines show the XAS spectra measured in the parallel (antiparallel) remanent magnetization state of the magnetite film without external field. (b) Solid ($I^+ - I^-$) and dotted ($\sum I_{\text{XMCD}}/\sum I^{\text{ISO}}$) lines represent the XMCD and its integrated spectrum normalized to the isotropic energy-integrated x-ray absorption.

and $J_{\|} = -0.025$ meV, which is considerably lower than the observed values. This rules out that the experimental result can simply be explained by dipolar coupling.

In summary, we demonstrate a strongly anisotropic exchange coupling possibly augmented by a dipolar component between the single unpaired spin of the central Cu(II) ion of a porphyrin molecule and the magnetite(100) surface. We propose that the anisotropic coupling results from the competition between ferromagnetic superexchange along Fe-N-Cu [14] and antiferromagnetic superexchange along Fe-O-Cu [11] with strength modified by the strong spin-orbit coupling [1]. The present experiment on a strongly heterogeneous system was designed to disentangle the anisotropic exchange coupling from crystalline magnetic anisotropy due to anisotropic bonding structures. Nevertheless, our results suggest that anisotropic exchange coupling may play an important role in many molecular magnetic systems, although it will often show up as an anisotropic magnetization behavior in homogeneous materials. For a dominant anisotropic coupling strength, the conventional Heisenberg model, usually used to describe exchange interaction in molecular magnets, becomes inapplicable. The interplay of the exchange interaction with the magnetization direction opens a new pathway to control the spin configuration in single molecular magnets.

This work was supported by the MAINZ Graduate School of Excellence (J. K.), by COMATT, and by the Deutsche Forschungsgemeinschaft (SFB/TRR 49). ANKA Angströmquelle Karlsruhe is acknowledged for the provision of beam time. We thank the MPI-IS Stuttgart for use of their XMCD end station at WERA.

*elmers@uni-mainz.de

[1] A. Palii, B. Tsukerblat, S. Klokishner, K. R. Dunbar, J. M. Clemente-Juan, and E. Coronado, Chem. Soc. Rev. **40**, 3130 (2011).
[2] A. Candini, G. Lorusso, F. Troiani, A. Ghirri, S. Carretta, P. Santini, G. Amoretti, C. Muryn, F. Tuna, G. Timco, E. J. L. McInnes, R. E. P. Winpenny, W. Wernsdorfer, and M. Affronte, Phys. Rev. Lett. **104**, 037203 (2010).
[3] D. Gatteschi and R. Sessoli, J. Magn. Magn. Mater. **272-276**, 1030 (2004).
[4] F. Meier, J. Levy, and D. Loss, Phys. Rev. B **68**, 134417 (2003).
[5] C. Schlegel, J. van Slageren, M. Manoli, E. K. Brechin, and M. Dressel, Phys. Rev. Lett. **101**, 147203 (2008).
[6] M. Urdampilleta, S. Klyatskaya, J. P. Cleuziou, M. Ruben, and W. Wernsdorfer, Nat. Mater. **10**, 502 (2011).
[7] A. Lodi Rizzini, C. Krull, T. Balashov, J. J. Kavich, A. Mugarza, P. S. Miedema, P. K. Thakur, V. Sessi, S. Klyatskaya, M. Ruben, S. Stepanow, and P. Gambardella, Phys. Rev. Lett. **107**, 177205 (2011).
[8] T. Suzuki, M. Kurahashi, and Y. Yamauchi, J. Phys. Chem. B **106**, 7643 (2002).
[9] A. Scheybal, T. Ramsvik, R. Bertschinger, M. Putero, F. Nolting, and T. A. Jung, Chem. Phys. Lett. **411**, 214 (2005).
[10] C. Iacovita, M. V. Rastei, B. W. Heinrich, T. Brumme, J. Kortus, L. Limot, and J. P. Bucher, Phys. Rev. Lett. **101**, 116602 (2008).
[11] M. Bernien, J. Miguel, C. Weis, M. E. Ali, J. Kurde, B. Krumme, P. M. Panchmatia, B. Sanyal, M. Piantek, P. Srivastava, K. Baberschke, P. M. Oppeneer, O. Eriksson, W. Kuch, and H. Wende, Phys. Rev. Lett. **102**, 047202 (2009).
[12] S. Javaid, M. Bowen, S. Boukari, L. Joly, J. B. Beaufrand, X. Chen, Y. J. Dappe, F. Scheurer, J. P. Kappler, J. Arabski, W. Wulfhekel, M. Alouani, and E. Beaurepaire, Phys. Rev. Lett. **105**, 077201 (2010).
[13] C. Waeckerlin, D. Chylarecka, A. Kleibert, K. Müller, C. Iacovita, F. Nolting, T. A. Jung, and N. Ballav, Nat. Commun. **1**, 61 (2010).
[14] H. Wende, M. Bernien, J. Luo, C. Sorg, N. Ponpandian, J. Kurde, J. Miguel, M. Piantek, X. Xu, P. Eckhold, W. Kuch, K. Baberschke, P. M. Panchmatia, B. Sanyal, P. M. Oppeneer, and O. Eriksson, Nat. Mater. **6**, 516 (2007).
[15] R. Prabakaran, R. Kesavamoorthy, G. L. N. Reddy, and F. P. Xavier, Phys. Status Solidi B **229**, 1175 (2002).
[16] E. Koch, Y. Jugnet, and F. Himpsel, Chem. Phys. Lett. **116**, 7 (1985).
[17] G. Dufour, C. Poncey, F. Rochet, H. Roulet, S. Iacobucci, M. Sacchi, F. Yubero, N. Motta, M. N. Piancastelli, A. Sgarlata, and M. D. Crescenzi, J. Electron Spectrosc. Relat. Phenom. **76**, 219 (1995).
[18] S. Carniato, Y. Luo, and H. Ågren, Phys. Rev. B **63**, 085105 (2001).
[19] O. V. Molodtsova, M. Knupfer, V. V. Maslyuk, D. V. Vyalikh, V. M. Zhilin, Y. A. Ossipyan, T. Bredow, I. Mertig, and V. Yu. Aristov, J. Chem. Phys. **129**, 154705 (2008).
[20] P. L. Cook, W. Yang, X. Liu, J. M. Garcia-Lastra, A. Rubio, and F. J. Himpsel, J. Chem. Phys. **134**, 204707 (2011).
[21] S. Stepanow, A. Mugarza, G. Ceballos, P. Moras, J. C. Cezar, C. Carbone, and P. Gambardella, Phys. Rev. B **82**, 014405 (2010).
[22] E. Stavitski and F. M. F. de Groot, Micron **41**, 687 (2010).
[23] I. Biswas, H. Peisert, M. B. Casu, B. E. Schuster, P. Nagel, M. Merz, S. Schuppler, and T. Chasse, Phys. Status Solidi A **206**, 2524 (2009).
[24] P. Carra, B. T. Thole, M. Altarelli, and X. Wang, Phys. Rev. Lett. **70**, 694 (1993).
[25] See Supplemental Material at http://link.aps.org/supplemental/10.1103/PhysRevLett.110.137202 for XAS and XMCD data measured at the Fe $L_{3,2}$ edges.
[26] P. Bruno, Phys. Rev. B **39**, 865 (1989).
[27] O. Sipr, J. Minar, and H. Ebert, Europhys. Lett. **87**, 67007 (2009).
[28] R. Pentchava, W. Moritz, J. Rundgren, S. Frank, D. Schrupp, and M. Scheffler, Surf. Sci. **602**, 1299 (2008).